REVIEW

Check for updates

Journal of
Sensor Science and Technology

The Korean Sensors Society

Advances in Raman Spectroscopic Detection of Pesticide Residues: Focus on Substrate Innovations

Hyunjun Park[1], Woochang Kim[1], Kyunghwan Chai[2], Gayoung Kim[2], Chaeyeong Kang[3], and Jinsung Park[1,3,+]

[1]*Department of Biomechatronics Engineering, Sungkyunkwan University, Suwon 16419, Republic of Korea*
[2]*Department of Biopharmaceutical Convergence, Sungkyunkwan University, Suwon 16419, Republic of Korea*
[3]*Department of MetaBiohealth, Sungkyunkwan University, Suwon 16419, Republic of Korea*

Cite This: *J. Sens. Sci. Technol. Vol. 34, No. 4 (2025) 387-397*

https://doi.org/10.46670/JSST.2025.34.4.387

ABSTRACT: The widespread use of pesticides in agriculture has significantly improved crop yields and pest control. However, the persistence of residual pesticides in food, soil, and water poses major risks to human health and the environment. Conventional detection methods, such as gas chromatography–mass spectrometry and liquid chromatography–mass spectrometry, provide high accuracy but are typically limited by complex sample preparation, long analysis times, and poor field applicability. In this context, Raman spectroscopy, particularly surface-enhanced Raman scattering (SERS), has emerged as a promising alternative for the rapid, sensitive, and nondestructive detection of pesticide residues. This review focuses on recent advances in the SERS-based detection of major pesticide residues (chlorpyrifos, thiram, and thiabendazole), which are frequently found in agricultural products and environmental samples. We highlight the fundamental principles of Raman scattering and SERS and introduce the mechanisms of signal enhancement via nanostructured substrates. Special emphasis is placed on the progressive development of high-performance SERS substrates, such as nanoparticle-decorated surfaces, hybrid bimetallic nanostructures, and 3D architectures, which significantly improve sensitivity, reproducibility, and stability. Finally, we discuss current challenges and future perspectives for translating SERS-based techniques into robust field-deployable systems for environmental monitoring and food safety assurance.

KEYWORDS: *Surface-enhanced Raman scattering (SERS), Pesticide residue detection, Advanced SERS substrate, Environmental monitoring*

1. INTRODUCTION

The continuous growth of the global population has led to increased pesticide use for improving agricultural productivity [1]. Pesticides play a critical role in pest control and crop yield enhancement. However, the presence of pesticide residues in agricultural products and the environment has raised significant health and environmental concerns, as reported in numerous studies [2]. Pesticide residues can accumulate in the human body through food intake. Long-term exposure to pesticides has been associated with severe adverse effects including carcinogenicity, neurological disorders, and endocrine disruption [3,4]. Chlorpyrifos (CPF), thiram, and thiabendazole (TBZ) are widely detected pesticide residues domestically and internationally. Strict maximum residue limits have been globally established owing to their toxicity and potential health risks [5,6]. Despite the enforcement of these limits, there are unresolved issues such as the misuse and overuse of pesticides, unintended environmental contamination, and introduction of pesticide residues during distribution processes. Therefore, the monitoring of pesticide residues is a critical public health and food safety concern.

The standard methods for pesticide residue detection rely on chromatographic techniques combined with mass spectrometry, such as gas chromatography–mass spectrometry, liquid chromatography–mass spectrometry, and high-performance liquid chromatography. Although these methods provide high precision and reliability, they require complex sample preparation, long analysis times, and high operational costs [7,8]. These methods are unsuitable for rapid on-site detection and real-time monitoring. Simplified approaches have been developed to address these limitations, such as immunoassays and

[+]Corresponding author: nanojspark@skku.edu
Received : Jun. 29, 2025, Revised : Jul. 8, 2025, Accepted : Jul. 16, 2025

colorimetric methods. However, they do not exhibit sufficient sensitivity, selectivity, and reproducibility and cannot fully replace the established methods.

Raman spectroscopy, which is based on the unique vibrational modes of molecules, provides a nondestructive analytical platform that enables qualitative and quantitative analyses with minimal sample preparation and short analysis times [9]. This technique has significant potential to overcome the aforementioned limitations, and it can be a viable alternative to conventional detection methods. Surface-enhanced Raman scattering (SERS) can amplify Raman signals by several orders of magnitude, thereby enabling the highly sensitive detection of trace-level pesticide residues. SERS-based pesticide residue monitoring has emerged as a promising solution owing to its advantages such as rapid analysis, label-free detection, and compatibility with field-deployable systems. Recent studies have demonstrated that SERS platforms can detect various pesticides, including CPF, thiram, and TBZ, at extremely low concentrations [10-12].

The key to achieving high-performance Raman-based detection is the development of efficient SERS substrates that can maximize signal enhancement. Noble-metal nanoparticles and nanostructures, particularly those based on gold (Au) and silver (Ag), have been widely employed in the early stages. In recent years, substrate design has evolved to improve signal reproducibility, chemical stability, and detection reliability [13,14]. This review summarizes the evolution of SERS substrate development strategies and comprehensively analyzes recent advances in pesticide residue detection, with focus on CPF, thiram, and TBZ.

2. TOXICITY OF PESTICIDE RESIDUES

2.1 CPF

CPF is an organophosphate pesticide that is widely used in agriculture to control various insect pests. Despite its effectiveness in crop protection, CPF has been subject to increasing regulatory scrutiny owing to its potential toxicity to humans and the environment. Its mechanism of action involves the inhibition of acetylcholinesterase, which is an essential enzyme in the nervous system [15,16]. Prolonged or acute exposure to CPF can disrupt cholinergic neurotransmission and lead to neurotoxicity, developmental disorders, and behavioral abnormalities, particularly in vulnerable populations such as children and pregnant women [17,18].

Multiple studies have linked prenatal exposure to CPF to adverse neurodevelopmental outcomes, including reduced IQ, attention deficits, and motor delays. These findings have prompted regulatory bodies in several countries, including the European Union and United States, to restrict or ban the use of CPF in food production and residential environments [19].

CPF persists in soil and water, where it poses ecotoxicological risks to nontarget organisms such as aquatic invertebrates, pollinators, and birds. Owing to the high bioaccumulation potential and low water solubility of CPF, CPF residues can enter the food chain and affect human health through dietary exposure.

Based on these toxicological and ecological risks, the sensitive and selective detection of CPF residues in food and environmental samples has become an important analytical challenge. Advanced detection platforms, such as SERS-based sensors, provide promising solutions for real-time monitoring at trace levels, which is critical for ensuring food safety and environmental protection.

2.2 Thiram

Thiram is a dithiocarbamate fungicide that is extensively used in agriculture to prevent fungal infections in seeds, fruits, and vegetables. Despite its effectiveness as a preventive agent, thiram poses notable health and ecological risks; this has led to ongoing evaluation by regulatory agencies [20].

Thiram interferes with cellular oxidative balance and enzyme function, particularly by inhibiting key sulfhydryl-containing enzymes. Acute exposure in humans can cause skin and eye irritation, headaches, nausea, and respiratory distress, whereas chronic exposure is associated with reproductive toxicity, liver and kidney damage, and potential neurotoxic effects [21].

Exposure to thiram occurs primarily through the consumption of contaminated food or occupational contact during pesticide spraying. Thiram is moderately mobile and can leach into the soil and water, thereby posing a risk to aquatic life. It is particularly toxic to fish and aquatic invertebrates and affects nontarget terrestrial species such as birds and pollinators. Although it is relatively unstable in sunlight and tends to degrade more rapidly than other pesticides, its transformation products may retain biological activity and contribute to the cumulative environmental burden [22].

Given its toxicity at low concentrations and environmental persistence, the development of sensitive detection methods for thiram residues in food and environmental matrices is essential.

2.3 TBZ

TBZ is a benzimidazole-class fungicide and anthelmintic agent that is widely used to control mold, blight, and rot in post-harvest crops such as citrus fruits, bananas, and potatoes [23-25]. It is also used in veterinary and human medicine to

treat parasitic worm infections. Although the acute toxicity of TBZ is generally lower than that of numerous other pesticides, concerns remain regarding its long-term exposure effects and metabolic persistence, which may pose significant toxicological and environmental risks [26-29].

In humans, therapeutic doses of TBZ are typically considered safe. However, excessive or prolonged exposure is associated with elevated hepatic enzyme levels, gastrointestinal disturbances, and potential neurotoxic effects [30,31].

Owing to the widespread use of TBZ in post-harvest treatment, TBZ residues are frequently found on fruits and vegetables. Thus, dietary intake is the primary route of human exposure to TBZ, particularly in populations with high consumption of treated produce.

TBZ can leach into the soil and aquatic ecosystems, where it exhibits moderate toxicity to nontarget organisms such as algae, daphnids, and fish. Although its environmental persistence is generally lower than that of organophosphates, its broad-spectrum biocidal properties raise concerns regarding unintended impacts on beneficial species including soil microbes and pollinators. These risks highlight the importance of the routine monitoring of residues to ensure food safety and environmental protection.

3. PRINCIPLE OF RAMAN SCATTERING AND SURFACE-ENHANCED RAMAN SCATTERING

3.1 Basic concept of Raman scattering

Raman spectroscopy is a nondestructive analytical technique that utilizes the energy-level differences caused by light scattering by a material to determine its molecular structure and chemical properties. The Raman scattering effect was first experimentally observed in 1928 by Indian physicists C.V. Raman and K.S. Krishnan [32]. Since then, Raman spectroscopy has been widely recognized as a powerful analytical method because of its ability to provide unique molecular fingerprints for various materials [33,34].

As illustrated in Fig. 1 (a), several types of light scattering can occur when a monochromatic laser beam is directed at a target molecule. Elastic scattering (Rayleigh scattering) occurs when the energy of scattered light is similar to that of incident light. However, inelastic scattering (Raman scattering) occurs when scattered light exhibits an energy shift compared with incident light. Stokes Raman scattering occurs when the energy of a scattered photon is lower than that of an incident photon, and anti-Stokes Raman scattering occurs when the energy of a scattered photon is higher than that of an incident photon.

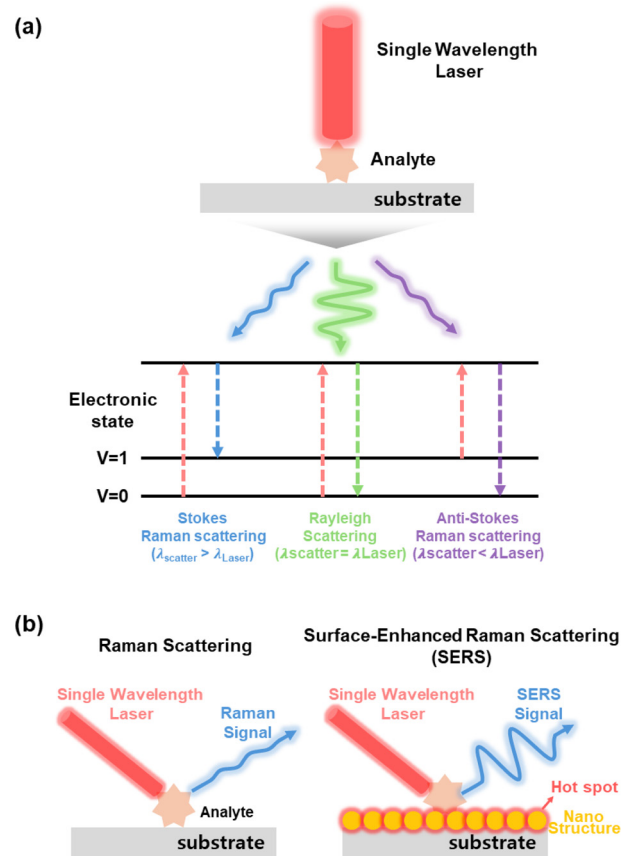

Fig. 1. Schematic diagram of the concept of Raman scattering and SERS. Basic mechanisms of (a) Raman scattering and (b) SERS.

In Stokes Raman scattering, the incident photon transfers a portion of its energy to the molecule, thereby exciting it from its ground vibrational state to a higher vibrational state. As a result, the scattered photon has lower energy (longer wavelength) compared with the incident photon. Stokes scattering generally dominates the Raman spectrum because most molecules exist in their ground vibrational states (v = 0) at room temperature.

In contrast, anti-Stokes Raman scattering occurs when the molecule is initially in an excited vibrational state and transfers energy to the scattered photon. This results in a scattered photon with higher energy (shorter wavelength) compared with the incident photon. As the population of molecules in excited vibrational states is significantly lower under ambient conditions, anti-Stokes signals are typically considerably weaker than Stokes signals [35].

Similarly, the energy difference between incident and scattered photons directly corresponds to the specific vibrational energy levels of a molecule, leading to a characteristic Raman spectrum that serves as a molecular fingerprint. On this basis, Raman spectroscopy can be used to identify molecular struc-

tures and monitor chemical interactions without complex labeling or extensive sample preparation. These fundamental principles form the basis for the widespread application of Raman spectroscopy in the chemical, biological, and environmental fields.

3.2 SERS mechanism

Raman spectroscopy is a highly versatile analytical technique used in numerous scientific and industrial fields. Despite its valuable analytical capability, Raman scattering is an intrinsically weak phenomenon, where approximately one in every 10^8 incident photons experience Raman scattering. This efficiency is approximately six to ten orders of magnitude lower than that of fluorescence. This substantially limits the sensitivity of Raman scattering in conventional applications.

SERS has been developed to overcome this fundamental limitation. SERS significantly amplifies the Raman signals of the molecules that are adsorbed onto nanostructured metallic surfaces, particularly those composed of noble metals such as Ag and Au. This phenomenon was first documented by Fleischmann et al., who reported a significant enhancement in the Raman signal of pyridine molecules on a roughened Ag electrode [36]. This finding led to extensive research that ultimately identified two principal mechanisms of the SERS effect: electromagnetic and chemical enhancement. A conceptual illustration of the Raman scattering and SERS mechanisms is shown in Fig. 1 (b).

The electromagnetic enhancement mechanism is primarily driven by the excitation of surface plasmons when light interacts with metallic nanostructures. Surface plasmons refer to the collective oscillations of conduction electrons on the surfaces of metals, which can strongly couple with incident light at specific resonance frequencies. When the frequency of incident light matches the surface plasmon resonance of metal nanoparticles, intense localized electromagnetic fields are generated close to the particle surface [37]. These concentrated fields, particularly within hot spots (nanoscale junctions or crevices between particles), can theoretically amplify a Raman signal by up to 10^{10} times, thereby making this mechanism the dominant contributor to the SERS effect.

Chemical enhancement also plays a significant role in SERS. This mechanism involves direct physicochemical interactions between an analyte and metallic substrate, which are typically facilitated by charge transfer between a molecule and metal surface. The polarizability of the molecule is altered because of this interaction, which increases its Raman scattering cross section. When the molecule is adsorbed onto the metal surface, the change in its polarizability is more than that when it is freely dispersed, leading to a noticeable amplification of the Raman signal. Although the enhancement factor (typically between 10^2 and 10^4) is lower compared with electromagnetic enhancement, it can increase depending on the molecular system.

The synergistic combination of electromagnetic and chemical enhancement enables SERS to achieve exceptionally high sensitivity and selectivity, thereby allowing for the detection of trace-level analytes even in complex sample matrices. Moreover, the ability to produce unique Raman spectra, which are typically described as molecular fingerprints, supports label-free detection and precise molecular identification. These characteristics make SERS particularly suitable for real-time monitoring and in-situ chemical analysis.

Note that the design and fabrication of SERS substrates are critical for maximizing the enhancement effect. Key factors, such as the size, shape, interparticle spacing, and surface morphology of metallic nanostructures, must be carefully engineered to optimize the electromagnetic field strength and efficiency of chemical interactions. The performance of an SERS-based detection platform strongly depends on the quality and reproducibility of the substrate, which is a key topic in the advancement of the SERS technology.

3.3 Substrates for maximizing SERS effect

Research on SERS substrates has evolved through innovative approaches including the fabrication of nanostructures that enhance local electromagnetic fields and the use of bimetallic combinations to utilize synergistic plasmonic effects [38]. Fig. 2 shows a range of SERS substrates based on these principles.

Nanoparticle-based substrates have played a key role in the advancement of the SERS technology. Metallic nanoparticles can generate strong localized electromagnetic fields through surface plasmon resonance, which significantly amplifies inherently weak Raman signals. Furthermore, nanoparticles provide a large active surface area for molecular adsorption owing to their high surface-to-volume ratio, thus enabling the highly sensitive detection of trace analytes.

For instance, spherical Au nanoparticles (GNPs) (Fig. 2 (a)) are chemically stable and can be easily functionalized with various compounds, including biomolecules, thereby making them ideal for the selective detection of low-concentration targets. GNPs with spiked or roughened surfaces (Thuja fruit-like nanoparticles, TFNPs) (Fig. 2 (b)) induce localized surface plasmon “hot spots” in the gaps between protrusions and further enhance the SERS effect without interparticle aggregation.

Bimetallic nanoparticles (BNPs), such as Au-core/Ag-shell structures (Fig. 2 (c)), have been developed to combine the advantages of the superior plasmonic enhancement of Ag and chemical stability of Au. These hybrid nanostructures exhibit

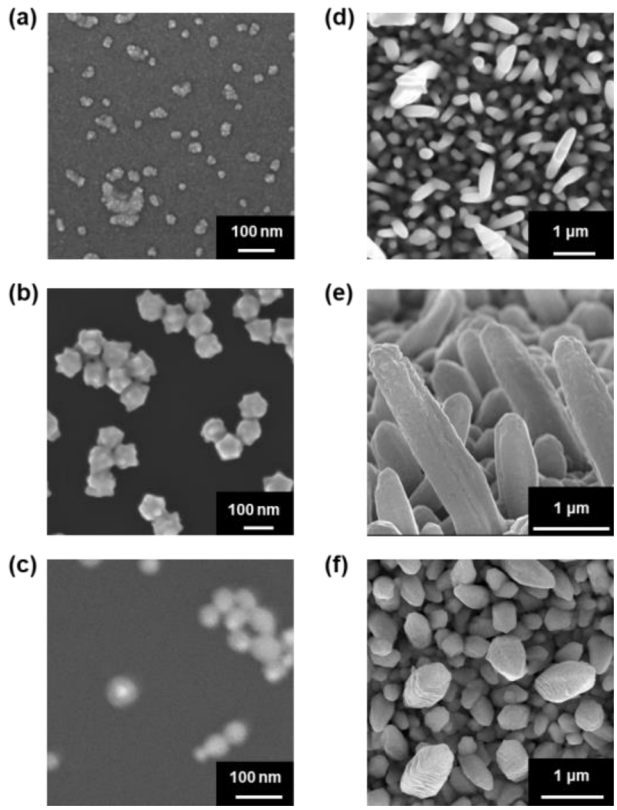

Fig. 2. Various nanoparticles and structures used as SERS substrates. SEM image of (a) GNPs, (b) TFNPs, (c) BNPs, (d) SNPis, (e) BNPis, and (f) nanocoral substrate.

tunable optical properties and are well suited for diverse SERS applications.

In addition to nanoparticles, nanostructure-based SERS substrates have attracted increasing attention because of their ability to generate uniform and reproducible signal enhancement. Unlike nanoparticle-based platforms, which typically confine hotspots to 2D surfaces, nanostructured substrates can create 3D architectures that generate dense and spatially distributed hot spots. This leads to improved signal amplification and reproducibility, thus providing broader potential for practical sensing applications.

An example of such a structure is Ag nanopillars (SNPi) (Fig. 2 (d)), which consist of vertically aligned and regularly spaced nanocolumns fabricated through electrochemical deposition using a three-electrode system. Based on this structure, Au@Ag bimetallic nanopillars (BNPi) (Fig. 2 (e)) have been synthesized through a galvanic replacement reaction, in which Au ions react with preformed Ag nanocolumns to form hybrid structures. These substrates have the combined advantages of columnar geometry and dual-metal composition, which significantly enhance SERS signals.

In recent years, coral-like nanocolumn substrates have been developed by codepositing Au and Ag ions and selectively etching Au using nitric acid, resulting in porous mixed-metal surfaces (nanocoral substrates) (Fig. 2 (f)). These structures maximize the number of hot spots and the surface contact area with target analytes, leading to superior SERS performance through bimetallic and surface roughness effects.

The progressive development of nanotechnology-based SERS substrates has provided new opportunities for ultrasensitive detection and monitoring in complex environments. These substrates are highly suitable for analyzing environmentally hazardous substances, including residual pesticides, which require sensitive and selective monitoring.

4. SERS-BASED RESIDUAL PESTICIDE DETECTION

4.1 CPF detection using SNPi substrate

A study has demonstrated the detection of CPF using an electrochemically fabricated SNPi substrate [39]. As shown in Fig. 3 (a), when an overpotential is applied to a Au-coated silicon (Si) substrate using a three-electrode system, Ag nanostructures grow and uniformly cover the surface to form vertically aligned SNPi structures; this is confirmed via scanning electron microscopy (SEM) imaging.

To evaluate the SERS performance of the SNPi substrate, bisphenol E (BPe), which is a representative Raman reporter molecule, is applied to three different substrates: a bare Si wafer, Au-coated substrate, and fabricated SNPi. The Raman spectra of BPe obtained for each substrate are shown in Fig. 3

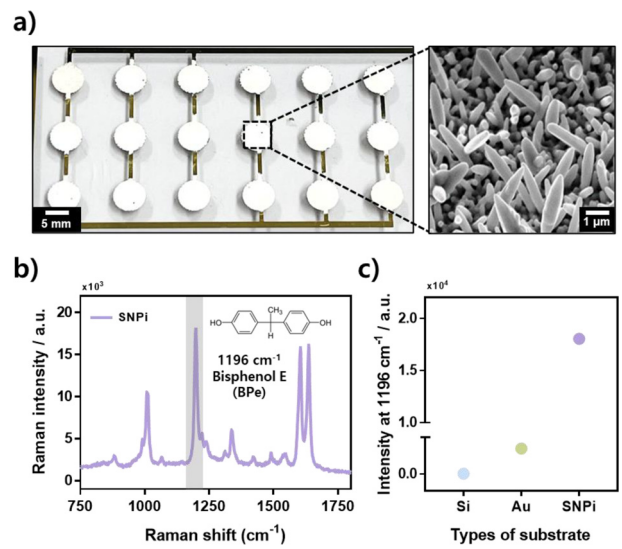

Fig. 3. Fabrication and performance evaluation of SNPi. (a) Actual shape of SNPi substrate (scale bar: 5 mm) and its SEM image. (b) Raman spectrum and molecular structure of BPe. (c) Comparison of Raman intensities at 1196 cm^{-1} after reaction of 1 mM BPe with Si, Au, and SNPi [40].

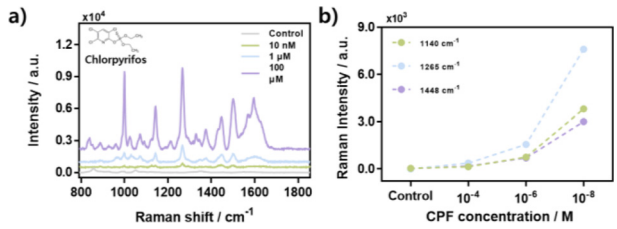

Fig. 4. Detection results of CPF using SNPi substrate. (a) Spectral results for CPF detection at different concentrations (100 μM, 1 μM, 10 nM) in SNPi. (b) Comparison of Raman intensities at different concentrations for specific Raman peaks of CPF (1140 cm^{-1}, 1265 cm^{-1}, 1448 cm^{-1}) [40].

(b). Among the characteristic peaks, the signal intensity at 1196 cm^{-1} is compared because of its high Raman activity. As illustrated in Fig. 3 (c), the SNPi substrate exhibits the highest Raman signal intensity, thus confirming its superior performance in SERS-based detection.

Based on the SERS performance of the SNPi substrate, a concentration-dependent detection study is conducted to evaluate its sensitivity for CPF detection. The analyte is tested at concentrations of 100 μM, 1 μM, and 10 nM, and the corresponding SERS spectra are shown in Fig. 4 (a). Among the characteristic Raman peaks of CPF, those at 1140 cm^{-1}, 1265 cm^{-1}, and 1448 cm^{-1} are selected for quantitative comparison. As shown in Fig. 4 (b), the Raman intensity of these peaks increases proportionally with the concentration, and CPF is clearly detected even at a low concentration of 10 nM.

This result highlights the capability of the platform for the ultrasensitive detection of CPF, which is difficult to detect at trace levels using conventional methods. Therefore, this study demonstrates the potential of the SNPi-based SERS substrate as a foundational technology for future applications in monitoring environmental toxicants using label-free and highly sensitive Raman spectroscopy [40].

4.2 Thiram detection using TFNPs@SNPi substrate

A study has proposed a hybrid SERS substrate that combines the previously discussed SNPi structure with nanoparticles to enhance the SERS effect [41]. Although the standalone 3D SNPi substrate provides strong signal enhancement owing to its vertically aligned nanostructures, it has a limitation in terms of the nonuniform hotspot distribution caused by structural irregularities. Metallic nanoparticles are incorporated into the system to overcome this limitation.

The nanoparticles effectively complement the uneven regions of the SNPi substrate, leading to the formation of uniformly distributed electromagnetic hotspots. TFNPs are used for this purpose because of their intrinsic hotspot-rich architecture. When combined with the SNPi substrate, these TFNPs significantly improve the overall SERS performance by introducing additional nanoscale hotspots and improving local field enhancement.

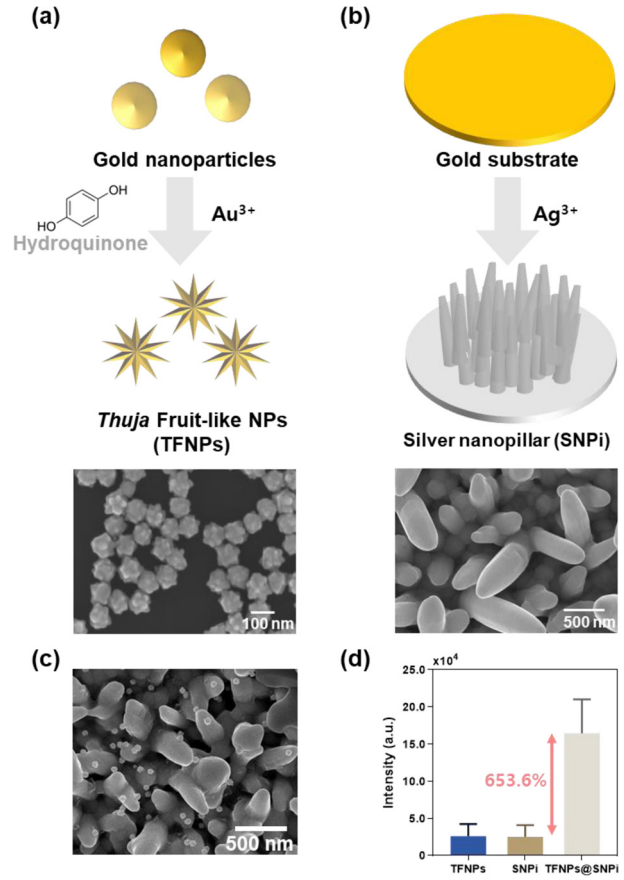

Fig. 5. Fabrication and performance evaluation of TFNPs@SNPi. (a) TFNPs fabricated by adding a reducing agent (hydroquinone) to spherical Au nanoparticles and their SEM image. (b) SNPi fabricated using electrochemical method and their SEM image. (c) Hybrid TFNPs@SNPi substrate fabricated by mixing the fabricated TFNPs and SNPis. (d) Raman intensity obtained after quantitative reaction of 4-ATP with TFNPs, SNPis, and TFNPs@SNPi [41].

TFNPs are synthesized by growing nanoscale Au protrusions on the surface of spherical Au nanoparticles through a controlled reduction reaction using hydroquinone as the reducing agent and $HAuCl_4$ as the Au precursor. This process creates a rough and uneven surface morphology, which contributes to the generation of numerous SERS-active hotspots. A schematic of the synthesis process is presented in Fig. 5 (a). The optimal TFNP morphology, which is achieved by precisely controlling the reducing agent concentration and reaction time, is confirmed via SEM imaging.

The SNPi substrate is fabricated using the same procedure as that employed in the previous CPF detection study. A Au-coated glass slide is subjected to an applied overpotential of

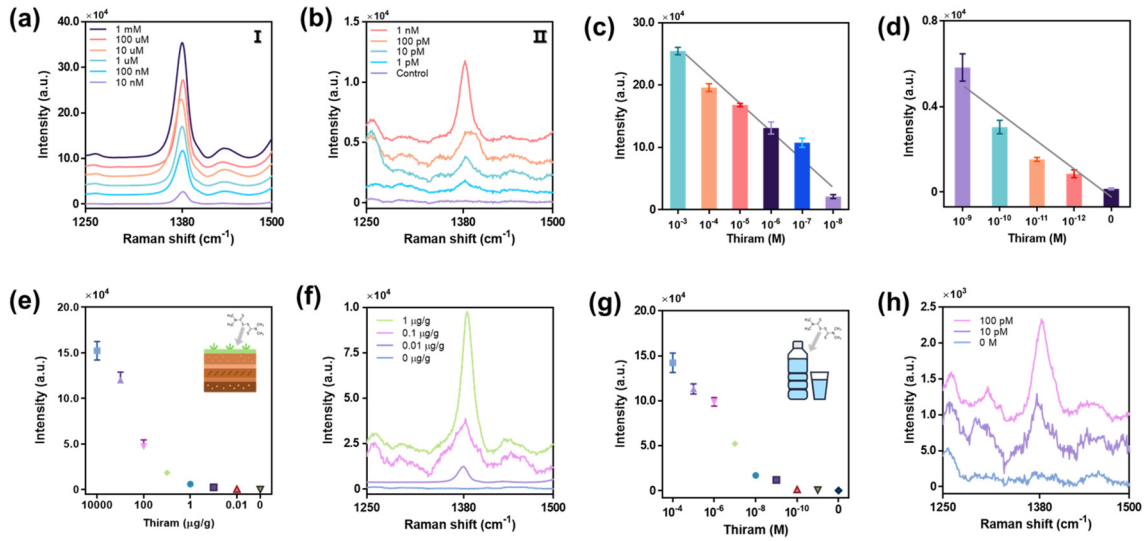

Fig. 6. Thiram detection results under various conditions using TFNPs@SNPi substrate. (a) Raman spectra around a specific peak (1380 cm^{-1}) of high-concentration thiram. (b) Raman spectra around a specific peak (1380 cm^{-1}) of low-concentration thiram. (c) Comparison of Raman intensities at 1380 cm^{-1} for high and (d) low concentrations of thiram. (e, f) Comparison of Raman intensities and spectra for different concentrations of thiram in soil. (g, h) Comparison of Raman intensities and spectra for different concentrations of thiram in drinking water [41].

-2 V in a three-electrode electrochemical system, which induces the vertical growth of Ag nanostructures. A schematic of the fabrication process is shown in Fig. 5 (b), and the corresponding SEM images confirm the successful formation of vertical SNPis.

The two components—TFNPs and SNPi—are integrated into a hybrid TFNPs@SNPi substrate using an optimized coupling strategy (Fig. 5 (c)). The SERS performance of the substrate is evaluated by applying 4-aminothiophenol (4-ATP), which a commonly used Raman reporter molecule, to the individual TFNP, SNPi, and hybrid TFNPs@SNPi substrates. The TFNPs@SNPi substrate exhibits a Raman signal enhancement of more than 653.6% compared with the individual components, thus demonstrating its superior SERS amplification capability (Fig. 5 (d)).

Based on the maximum enhancement in the performance of the TFNPs@SNPi hybrid substrate, its ability to detect thiram is systematically evaluated. Thiram solutions with various concentrations are applied to the substrate, and the corresponding Raman spectra are recorded. As shown in Fig. 6 (a), strong Raman signals are observed at 1380 cm^{-1}, which is a characteristic peak of thiram, in the high-concentration range. Even at lower concentrations, distinguishable signals are clearly observed at 1380 cm^{-1} compared with the control (Fig. 6 (b)).

Quantitative analysis shows that the Raman intensity at 1380 cm^{-1} increases proportionally with the thiram concentration (Figs. 6 (c) and (d)), and the limit of detection is experimentally determined to be 120 fM.

To assess the applicability of the substrate in real-world conditions, thiram is detected in complex matrices such as soil and water, where accidental pesticide leakage is likely to occur. For the soil analysis, garden soil is obtained from a local market and used without pretreatment to better mimic environmental conditions, including potential interfering substances. Soil–thiram mixtures are prepared by adjusting the mass of thiram mixed with 1 g of soil to achieve final concentrations of 0–10 mg/g. The Raman spectra of these samples are recorded, and the intensity at 1380 cm^{-1} is analyzed (Fig. 6 (e)). The detection limit of thiram in soil is calculated as 1.06 ng/g (Fig. 6 (f)).

Water is selected as another relevant medium because of its high exposure potential and direct implications for human and animal health. Thiram solutions with concentrations of 0–100 μM are prepared in distilled water. Similar to the previous experiments, the Raman intensities at 1380 cm^{-1} are measured (Fig. 6 (g)), and the detection limit is calculated to be as low as 762 fM (Fig. 6 (h)).

In summary, despite the presence of various interfering substances in environmental samples such as soil and water, the sensitivity of the TFNPs@SNPi-based SERS sensor is comparable to that achieved under controlled laboratory conditions. These findings highlight the potential of the platform for the practical and field-deployable monitoring of thiram residues, particularly in actual leakage scenarios.

4.3 TBZ detection using BNP@SNPi Substrate

A study has developed a hybrid BNP@SNPi SERS substrate, which incorporates Au@Ag BNPs into SNPis to

enhance the SERS effect [42]. This substrate retains the advantages of 3D-structured SNPis, such as a high surface area and vertical nanostructure-induced hotspot formation, while addressing their inherent limitation of nonuniform hotspot distribution through the functional integration of BNPs.

BNPs are strategically designed to combine the plasmonic characteristics of Au and Ag. Au nanoparticles exhibit plasmon resonance in the red-to-near-infrared region, whereas Ag shows strong plasmonic resonance in the visible range. BNPs combine these metals to provide a broadband plasmonic response, thereby enabling stronger and more efficient electromagnetic field enhancement under laser excitation compared with their single-metal counterparts. As a result, the BNP@SNPi substrate is expected to achieve the maximum SERS performance by leveraging the synergistic effects of bimetallic plasmon coupling and nanostructure-induced hotspot localization.

The BNPs are synthesized using Au nanoparticles as seeds, followed by the reduction of $AgNO_3$ with ascorbic acid to form a Ag shell around the Au core [43]. Well-defined Au-core/Ag-shell BNPs are fabricated through a series of optimization steps, and their morphologies are confirmed via SEM imaging (Fig. 7 (a)). Energy-dispersive X-ray spectroscopy (EDS) performed on transmission electron microscopy (TEM) images further validates the core–shell structure and clearly indicates that the core consists of Au and the outer shell is composed of Ag (Fig. 7 (b)).

The synthesized BNPs are subsequently functionalized onto the SNPi substrate to construct the hybrid BNP@SNPi SERS platform (Fig. 7 (c)). The SERS performance of the hybrid substrate is compared with those of the SNPi and GNP@SNPi substrates. 4-ATP (10 μM) is applied to each substrate, and the Raman intensity at the characteristic peak of 1076 cm^{-1} is measured. As shown in Fig. 7 (d), the BNP@SNPi substrate exhibits the highest signal intensity, which is attributed to the synergistic plasmonic enhancement due to the bimetallic BNPs and high-density hotspots within the 3D SNPi structure.

The concentration-dependent detection of 4-ATP is performed to validate the sensitivity of the substrate. As illustrated in Fig. 7 (e), the detection limit of the BNP@SNPi platform is as low as 103 fM, which demonstrates its excellent potential for ultratrace molecular sensing.

The ability of the BNP@SNPi substrate to detect TBZ is evaluated. As shown in Fig. 8 (a), the Raman spectra obtained for high and low concentrations of TBZ exhibit a strong characteristic peak at 782 cm^{-1}. The limit of detection is calculated as 1.06 pM (Fig. 8 (b)), which shows the exceptional sensitivity of the platform under laboratory conditions.

To further assess the practical applicability of the BNP@SNPi substrate, TBZ is detected in environmental water

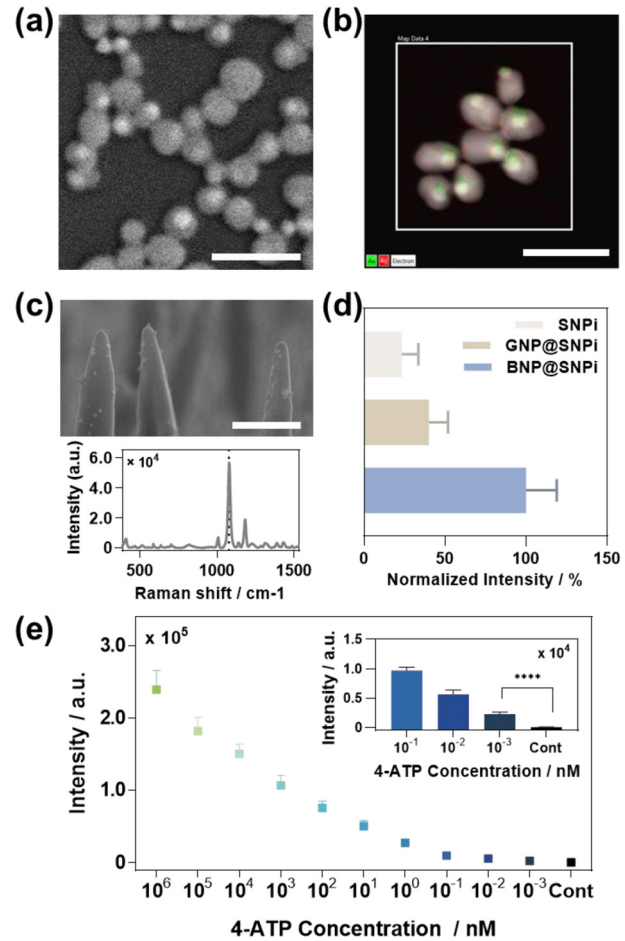

Fig. 7. Fabrication and performance evaluation of BNP@SNPi. (a) SEM image of BNPs. (b) TEM EDS and (c) SEM images of hybrid BNP@SNPi substrate and Raman spectrum obtained using 4-ATP (10 μM). (d) Comparison of Raman intensity at 1076 cm^{-1} after quantitative reaction of 4-ATP with SNPis, GNP@SNPis, and BNP@SNPis, respectively. (e) Raman performance evaluation through reaction of BNP@SNPi substrate with various concentrations of 4-ATP [42].

samples where TBZ contamination is plausible, i.e., tap water and drinking water. TBZ is widely used in agricultural cultivation, and its potential to leach into public water supplies poses a concern. TBZ-spiked tap water samples are prepared at various concentrations and reacted with the BNP@SNPi substrate. The resulting Raman intensities at 782 cm^{-1} in the low-concentration range are shown in Fig. 8 (c). A detection limit of 146.5 pM is calculated from these data, thus confirming the high sensitivity of the system in realistic aqueous matrices.

A similar approach is applied to drinking water samples, and the BNP@SNPi platform exhibits reliable detection performance. After the reaction of the TBZ solutions and substrate and the analysis of the Raman intensity at 782 cm^{-1}, a statistically significant signal is observed in the low-concentration range (confirmed via t-test), and the limit of detection is 245.5

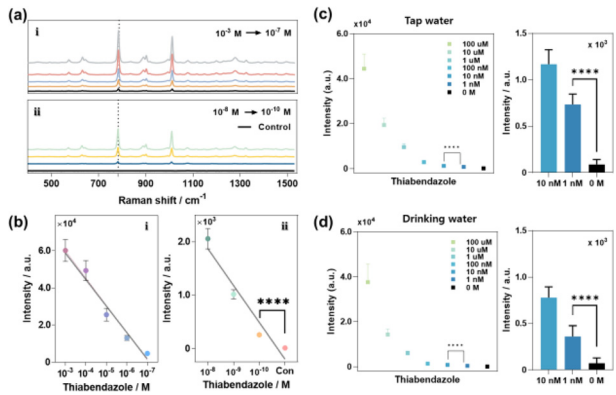

Fig. 8. TBZ detection results under various conditions using BNP@SNPi substrate. (a) Raman spectra obtained at i) high and ii) low concentrations of TBZ. (b) Comparison of Raman intensity at 782 cm^{-1}. (c) TBZ detection results for different concentrations based on tap water (actual environmental sample) and comparison of Raman intensities at 782 cm^{-1}. (d) TBZ detection results for different concentrations based on drinking water and comparison of Raman intensities at 782 cm^{-1} [42].

pM (Fig. 8 (d)).

These results highlight the high sensitivity and wide dynamic range of the BNP@SNPi SERS platform. The detection limits represent a few of the most sensitive TBZ detection results achieved using Raman-based techniques until now. This highlights the potential of the hybrid substrate for practical applications in environmental monitoring and food safety.

5. CONCLUSIONS

The increasing concern over environmental toxicants, particularly residual pesticides, in food and agricultural systems highlights the urgent requirement for highly sensitive, rapid, and reliable detection technologies. Despite the widespread use and regulatory monitoring of pesticides such as CPF, thiram, and TBZ, they continue to pose significant health and ecological risks owing to their persistence, bioaccumulation, and potential for chronic toxicity. As conventional analytical methods typically have complex instrumentation, labor-intensive sample preparation, and limited on-site applicability, there is an increasing demand for more versatile and field-deployable alternatives.

Raman spectroscopy, particularly SERS, has emerged as a powerful analytical approach for overcoming these challenges. SERS is used to quantify trace contaminants in complex matrices by providing molecule-specific spectral fingerprints with ultrahigh sensitivity and label-free detection capabilities. The core of this technique lies in the continuous evolution of SERS substrates, which amplify Raman signals by engineering localized surface plasmon effects and optimizing molecular interactions.

This review highlights the progressive development of various SERS substrates, which range from nanoparticle-based platforms to 3D nanostructures and hybrid bimetallic systems. These innovations have significantly improved the signal uniformity, reproducibility, and enhancement factors. Note that recent studies have successfully detected multiple pesticide residues, including CPF, thiram, and TBZ, at extremely low concentrations in laboratory and real-world sample matrices such as soil, water, and food.

The integration of advanced nanofabrication techniques with SERS provides a promising approach for developing next-generation sensing platforms for environmental monitoring. As substrate design becomes more sophisticated, the potential for real-time on-site pesticide detection in agricultural, food safety, and ecological applications continues to expand. Future efforts should focus on translating these high-performance substrates into robust commercial devices to ensure analytical rigor and accessibility for widespread environmental use.

CRediT Authorship Contribution Statement

Hyunjun Park: Conceptualization, Writing – original draft. **Woochang Kim:** Conceptualization, Investigation, Project administration. **Kyunghwan Chai:** Visualization, Software. **Gayoung Kim:** Methodology, Formal analysis. **Chaeyeong Kang:** Data curation, Validation. **Jinsung Park:** Supervision, Writing – review and editing.

Declaration of Competing Interest

The authors declare that they have no known competing financial interests or personal relationships that could have appeared to influence the work reported in this paper.

Acknowledgements

This research was funded by the National Research Foundation of Korea (NRF) under Grant Nos. NRF-2023R1A2C2004964, RS-2024-00438542, and RS-2025-00554830.

REFERENCES

[1] S. Ali, M.I. Ullah, A. Sajjad, Q. Shakeel, A. Hussain, Environmental and health effects of pesticide residues, In: E. Lichtfouse, Sustainable agriculture reviews, Springer, Cham, Switzerland, 2021, pp. 311–336.
[2] C.M. Raffa, F. Chiampo, Bioremediation of agricultural soils polluted with pesticides: A review, Bioengineering 8 (2021) 92.
[3] M. Bilal, H.M. Iqbal, D. Barceló, Persistence of pesticides-based contaminants in the environment and their effective degradation using laccase-assisted biocatalytic systems, Sci.

Total Environ. 695 (2019) 133896.
[4] L. Parra-Arroyo, R.B. González-González, C. Castillo-Zacarías, E.M.M. Martínez, J.E. Sosa-Hernández, M. Bilal, et al., Highly hazardous pesticides and related pollutants: Toxicological, regulatory, and analytical aspects, Sci. Total Environ. 807 (2022) 151879.
[5] S.Y. Foong, N.L. Ma, S.S. Lam, W. Peng, F. Low, B.H. Lee, et al., A recent global review of hazardous chlorpyrifos pesticide in fruit and vegetables: Prevalence, remediation and actions needed, J. Hazard. Mater. 400 (2020) 123006.
[6] European Food Safety Authority (EFSA), H. Abdourahime, M. Anastassiadou, A. Brancato, D. Brocca, L.C. Cabrera, et al., Review of the existing maximum residue levels for dazomet according to Article 12 of Regulation (EC) No 396/2005, EFSA J. 17 (2019) e05562.
[7] Y. Su, J. Lu, J. Liu, F. Li, N. Wang, H. Lei, et al., Optimization of a QuEChERS–LC–MS/MS method for 51 pesticide residues followed by determination of the residue levels and dietary intake risk assessment in foodstuffs, Food Chem. 434 (2024) 137467.
[8] L. Alder, K. Greulich, G. Kempe, B. Vieth, Residue analysis of 500 high priority pesticides: better by GC–MS or LC–MS/MS?, Mass Spectrom. Rev. 25 (2006) 838–865.
[9] C.J. Strachan, T. Rades, K.C. Gordon, J. Rantanen, Raman spectroscopy for quantitative analysis of pharmaceutical solids, J. Pharm. Pharmacol. 59 (2007) 179–192.
[10] Y. Shi, Y. Zhu, J. Sun, H. Yin, J. Yin, SERS detection of thiram using a 3D sea cucumber-like composite flexible porous substrate, Analyst 149 (2024) 5041–5051.
[11] D.T. Linh, Q.-D. Mai, D.T.N. Nga, N.T. Anh, H. Van Tuan, H.A. Nguyen, et al., Surface ligand modified silver nanoparticles-based SERS sensing platform for ultrasensitive detection of the pesticide thiram in green tea leaves: roles of coating agents in sensing performance, RSC Adv. 14 (2024) 9975–9984.
[12] S. Adhikari, R. Joshi, R. Joshi, M. Kim, Y. Jang, L.T. Tufa, et al., Rapid and ultrasensitive detection of thiram and carbaryl pesticide residues in fruit juices using SERS coupled with the chemometrics technique, Food Chem. 457 (2024) 140486.
[13] H.S. Kim, H.J. Kim, J. Lee, T. Lee, J. Yun, G. Lee, et al., Hand-held Raman spectrometer-based dual detection of creatinine and cortisol in human sweat using silver nanoflakes, Anal. Chem. 93 (2021) 14996–15004.
[14] K.S. Park, A. Choi, H.J. Kim, I. Park, M.-S. Eom, S.-G. Yeo, et al., Ultra-sensitive label-free SERS biosensor with high-throughput screened DNA aptamer for universal detection of SARS-CoV-2 variants from clinical samples, Biosens. Bioelectron. 228 (2023) 115202.
[15] M. Eddleston, Patterns and problems of deliberate self?poisoning in the developing world, Qjm 93 (2000) 715-731.
[16] D. Gunnell, M. Eddleston, M.R. Phillips, F. Konradsen, The global distribution of fatal pesticide self-poisoning: systematic review, BMC Public Health 7 (2007) 357.
[17] V.A. Rauh, R. Garfinkel, F.P. Perera, H.F. Andrews, L. Hoepner, D.B. Barr, et al., Impact of prenatal chlorpyrifos exposure on neurodevelopment in the first 3 years of life among inner-city children, Pediatrics 118 (2006) e1845-e1859.
[18] R.D. Burke, S.W. Todd, E. Lumsden, R.J. Mullins, J. Mamczarz, W.P. Fawcett, et al., Developmental neurotoxicity of the organophosphorus insecticide chlorpyrifos: from clinical findings to preclinical models and potential mechanisms, J. Neurochem. 142 (2017) 162–177.
[19] T.J. Centner, Cancelling pesticide registrations and revoking tolerances: The case of chlorpyrifos, Environ. Toxicol. Pharmacol. 57 (2018) 53–61.
[20] A.E. Larsen, S.D. Gaines, O. Deschênes, Agricultural pesticide use and adverse birth outcomes in the San Joaquin Valley of California, Nat. Commun. 8 (2017) 302.
[21] S. Salam, A. Arif, R. Mahmood, Thiram-induced cytotoxicity and oxidative stress in human erythrocytes: an in vitro study, Pestic. Biochem. Physiol. 164 (2020) 14–25.
[22] C. Sirtori, A. Agüera, I. Carra, J.A. Sanchéz Pérez, Identification and monitoring of thiabendazole transformation products in water during Fenton degradation by LC-QTOF-MS, Anal. Bioanal. Chem. 406 (2014) 5323–5337.
[23] G. Fu, D.-W. Sun, H. Pu, Q. Wei, Fabrication of gold nanorods for SERS detection of thiabendazole in apple, Talanta 195 (2019) 841–849.
[24] F.K. Alsammarraie, M. Lin, A. Mustapha, H. Lin, X. Chen, Y. Chen, et al., Rapid determination of thiabendazole in juice by SERS coupled with novel gold nanosubstrates, Food Chem. 259 (2018) 219–225.
[25] B. Gilbert-López, J.F. García-Reyes, M. Mezcua, A. Molina-Díaz, A.R. Fernández-Alba, Determination of post-harvest fungicides in fruit juices by solid-phase extraction followed by liquid chromatography electrospray time-of-flight mass spectrometry, J. Agric. Food Chem. 55 (2007) 10548–10556.
[26] G. Lankas, D. Wise, Developmental toxicity of orally administered thiabendazole in Sprague—Dawley rats and New Zealand white rabbits, Food Chem. Toxicol. 31 (1993) 199–207.
[27] A. Ogata, H. Ando, Y. Kubo, K. Hiraga, Teratogenicity of thiabendazole in ICR mice, Food Chem. Toxicol. 22 (1984) 509–520.
[28] Y. Tada, T. Fujitani, N. Yano, K. Yuzawa, A. Nagasawa, M. Yoneyama, Thiabendazole induces urinary tract toxicity in male ICR mice, Toxicology 162 (2001) 1–10.
[29] Y. Tada, T. Fujitani, N. Yano, K. Yuzawa, A. Nagasawa, N. Aoki, et al., Chronic toxicity of thiabendazole (TBZ) in CD-1 mice, Toxicology 169 (2001) 163–176.
[30] A. Mamane, I. Baldi, J.-F. Tessier, C. Raherison, G. Bouvier, Occupational exposure to pesticides and respiratory health, Eur. Respir. Rev. 24 (2015) 306–319.
[31] S. Salam, Z. Iqbal, A.A. Khan, R. Mahmood, Oral administration of thiram inhibits brush border membrane enzymes, oxidizes proteins and thiols, impairs redox system and causes histological changes in rat intestine: A dose dependent study, Pestic. Biochem. Physiol. 178 (2021) 104915.
[32] C.V. Raman, K.S. Krishnan, A new type of secondary radiation, Nature 121 (1928) 501–502.
[33] D.K. Pathak, C. Rani, A. Sati, R. Kumar, Developments in Raman Spectromicroscopy for Strengthening Materials and

Natural Science Research: Shaping the Future of Physical Chemistry, ACS Phys. Chem. Au 4 (2024) 430–438.
[34] R.S. Das, Y. Agrawal, Raman spectroscopy: Recent advancements, techniques and applications, Vib. Spectrosc. 57 (2011) 163–176.
[35] M. Prochazka, Basics of Raman scattering (RS) spectroscopy, In: B.S. Gerstman (Ed.), Surface-Enhanced Raman Spectroscopy: Bioanalytical, Biomolecular and Medical Applications, Springer, Switzerland, 2016, pp. 7–19.
[36] M. Fleischmann, P.J. Hendra, A.J. McQuillan, Raman spectra of pyridine adsorbed at a silver electrode, Chem. Phys. Lett. 26 (1974) 163–166.
[37] W. Hou, S.B. Cronin, A review of surface plasmon resonance?enhanced photocatalysis, Adv. Funct. Mater. 23 (2013) 1612–1619.
[38] J. Ding, M. Zhang, L. Kong, P. Song, Y. Yang, Fabrication of core–shell-like bimetallic SERS substrates with inter-coordination effect for catalysis of p-mercaptoaniline, Anal. Methods 16 (2024) 6563–6569.
[39] D. Bang, Y.W. Chang, J. Park, T. Lee, J. Park, J.-S. Yeo, et al., One-step electrochemical fabrication of vertically self-organized silver nanograss, J. Mater. Chem. A 1 (2013) 4851–4857.
[40] H. Park, J. Park, G. Lee, W. Kim, J. Park, Detection of chlorpyrifos using bio-inspired silver nanograss, Materials 15 (2022) 3454.
[41] W. Kim, G. Kim, H. Park, K. Chai, J. Park, J. Park, Detecting and tracking thiram in leakage pathways using bio-inspired nanograss with thuja fruit-like nanoparticles, Sens. Actuators B Chem. 406 (2024) 135405.
[42] H. Park, G. Kim, W. Kim, E. Park, J. Park, J. Park, Highly Sensitive and Wide-Range Detection of Thiabendazole via Surface-Enhanced Raman Scattering Using Bimetallic Nanoparticle-Functionalized Nanopillars, Biosensors 14 (2024) 133.
[43] E. Ferreira, B. Kharisov, A. Vázquez, E.A. Méndez, I. Severiano-Carrillo, M. Trejo-Durán, Tuning the nonlinear optical properties of Au@ Ag bimetallic nanoparticles, J. Mol. Liq. 298 (2020) 112057.

Hyunjun Park received his Ph.D. in Biomechatronics in 2025, and he is currently working as a biotechnology researcher (postdoctoral fellow) at Sungkyunkwan University. His research focuses on manufacturing advanced SERS substrates for the highly sensitive detection of environmental toxicants and biomarkers using Raman spectroscopy. His other interests include SERS data analysis using artificial techniques.

Jinsung Park is a professor at the Department of Bio-Mechatronic Engineering, Sungkyunkwan University, South Korea. He received his B.S. and Ph.D. degrees from the Department of Mechanical Engineering, Korea University, in 2007 and 2013, respectively. He completed a postdoctoral fellowship at the Korea University in 2013. His research focuses on the investigation of biomolecular interactions using atomic force microscopy, mechanical properties of biomolecules and nanostructures, surface potential measurements of biomolecules and nanomaterials using Kelvin probe force microscopy, and environmental nanotoxic material detection using various sensing methods. His other interests include the detection of toxic substances and biomolecules using electrochemical and SERS sensors.